Graphene on Ru(0001): Contact Formation and Chemical Reactivity on the Atomic Scale

S. J. Altenburg,[1,*] J. Kröger,[2] B. Wang,[3] M.-L. Bocquet,[3] N. Lorente,[4] and R. Berndt[1]

[1]*Institut für Experimentelle und Angewandte Physik, Christian-Albrechts-Universität zu Kiel, D-24098 Kiel, Germany*
[2]*Institut für Physik, Technische Universität Ilmenau, D-98693 Ilmenau, Germany*
[3]*Université de Lyon, Laboratoire de Chimie, Ecole Normale Supérieure de Lyon, CNRS, F69007 Lyon, France*
[4]*Centre d'Investigació en Nanociència i Nanotecnologia (CSIC-ICN), Campus de la UAB, E-08193 Bellaterra, Spain*

(Received 13 September 2010; published 29 November 2010)

Graphene on Ru(0001) is contacted with Au tips of a cryogenic scanning tunneling microscope. The formation and conductance of single-atom contacts vary within the moiré unit cell. Density functional calculations reveal that elastic distortions of the graphene lattice occur at contact due to a selectively enhanced chemical reactivity of C atoms at hollow sites of Ru(0001). Concomitant quantum transport calculations indicate that the graphene-Ru distance determines the conductance variations.

DOI: 10.1103/PhysRevLett.105.236101 PACS numbers: 68.65.Pq, 68.37.Ef, 72.80.Vp

Since the first reported preparation of freestanding graphene in 2004 [1], many strikingly unusual properties of this sp^2-hybridized two-dimensional carbon crystal have been unraveled. In particular, the extremely high charge carrier mobility, the possibility to achieve ballistic electron transport at room temperature, and the pronounced ambipolar electric field effect [1–4] make graphene a promising candidate as a material for future electronic devices. Graphene layers with a high degree of perfection may be grown on crystal surfaces, where the interaction with the substrate modifies its electronic properties to varying degrees [5–11]. On most transition metals superstructures occur and lead to periodic modulations of geometric, electronic, and bonding properties.

Here, we use a low-temperature scanning tunneling microscope (STM) to probe, with atomic precision, the conductance $G = I/V$ (I: current; V: sample voltage) of junctions comprising a Au tip and a single graphene layer on Ru(0001). On this substrate graphene forms a hexagonal moiré superstructure with a periodicity of ≈ 30 Å, which involves a buckling of the graphene sheet and a strongly inhomogeneous electronic structure [8,12–14]. Increased chemical reactivity in the strongly bound regions of the moiré superstructure has been shown by metal deposition, leading to cluster formation in these regions [15–17]. As these works addressed the final state of the reactions, they do not show the actual reaction path and the role of the chemically distinct components of the graphene sheet. Our STM measurements directly probe the chemical reactivity of graphene during bond formation and reveal its location on the atomic scale. This is possible owing to significant variations of the tip-graphene contact formation process and of the conductance within the moiré unit cell. A smooth transition from tunneling to contact occurs in regions where the graphene layer is buckled away from the substrate, while in the strongly bound parts a jump to contact is observed, similar to point contacts on pristine noble metal surfaces [18,19]. This behavior can be traced back to the different electronic structure and ultimately to the different chemical reactivity of the graphene layer as revealed by density functional theory (DFT).

Experiments were performed with a home-built STM, operated at 5.2 K and in ultrahigh vacuum. Ru(0001) surfaces were cleaned by Ar^+ bombardment and annealing. Graphene films were obtained by exposing the sample to 6×10^{-4} Pa s of ethene at room temperature and subsequent annealing to 1400 K. This procedure leads to a partial coverage of Ru(0001) by highly ordered graphene [see Fig. 1(a)]. Au tips were prepared by *ex situ* cutting, *in vacuo* heating, and Ar^+ bombardment. The tips were further formed by controlled contact to Ru(0001), thereby depositing Au from the tip apex onto the surface. This procedure was repeated until constant-current images of single deposited Au atoms were symmetric and sharp, and atomic resolution of graphene was reached, which indicates that the tip was terminated by a single atom. Contact

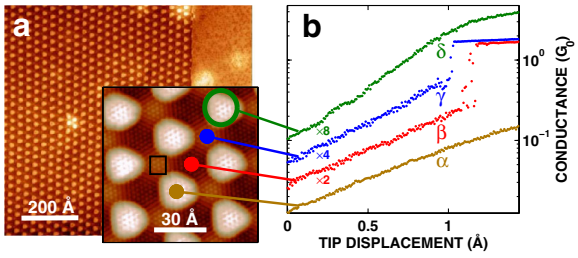

FIG. 1 (color online). (a) Constant-current STM image of graphene on Ru(0001) (100 mV, 0.1 nA) showing the moiré lattice (left-hand side) and a clean area of Ru(0001) (right-hand side). Inset: Atomically resolved image (40 mV, 300 nA). The black rectangle indicates the position in the moiré unit cell analyzed further below (Fig. 3). (b) Conductance versus tip displacement curves (sample voltage 100 mV), obtained at the indicated positions in the moiré unit cell. For clarity, curves β, γ, and δ have been multiplied by factors of 2, 4, and 8. In regions β and γ a sharp jump to contact is observed, with respective contact conductances of $0.8G_0$ and $0.43G_0$.

experiments were performed by displacing the tip towards the surface (positive displacement) and simultaneously measuring the current. Despite the high currents, no significant voltage drop occurred at the input impedance of the current-to-voltage converter [20]. Imaging of the contacted area prior to and after the contact ensured the absence of structural changes of the sample or tip.

Calculations were performed with the VASP [21] package based on DFT, which implements plane waves. The projector-augmented wave method [22,23] is adopted to accurately describe the valence electron-valence core interaction. The plane-wave kinetic-energy cutoff was set to 300 eV and the Brillouin zone was sampled with a single k point at its center. The exchange-correlation functional of Perdew, Burke, and Ernzerhof (PBE [24]) in the generalized gradient approximation framework was adopted. The supercell consisting of 661 atoms had a (11×11) lateral periodicity and contained one layer of (12×12) graphene deposited on top of a three-layer slab of Ru atoms. The tip cluster consisted of a pyramid containing 10 Au atoms and was mounted on the reverse side of the metallic slab, so that the graphene overlayer was contacted by the tip of the adjacent supercell in the normal direction. The tip-graphene interaction resulted from an extensive geometry optimization of the graphene and the tip cluster for a set of height values of the periodic supercell in the normal direction. The graphene layer, the uppermost Ru layer, and the Au tip were free to relax until the self-consistent forces reached 0.1 eV/Å.

As graphene on Ru(0001) forms a moiré superstructure [9] (a high region α and two inequivalent low regions β and γ), conductance measurements are performed at different locations in the moiré unit cell (Fig. 1). While in α both C atoms of the graphene unit cell are visible in STM images [25], in β and γ only the C atoms at fcc and hcp sites of Ru(0001) show contrast. The corrugation of the graphene film leads to varying graphene-Ru distances. According to calculations [25], these distances are 3.7 Å, 2.2 Å, and 2.3 Å in α, β, and γ, respectively.

Conductance data are displayed in Fig. 1(b). In region α the conductance changes smoothly from tunneling to contact. The conductance at contact never rises above an exponential extrapolation of the tunneling conductance at small displacements. Moreover, the conductance values observed here are the lowest within the moiré unit cell and typically do not exceed $0.3G_0$ ($G_0 = 2e^2/h$, e: electron charge; h: Planck's constant), provided the tip is atomically sharp and the tip approach is stopped before inelastic deformations occur. In contrast, in the β and γ regions an abrupt jump from tunneling to contact is found. The contact conductance of the β region varies between $0.4G_0$ and $0.8G_0$, while larger values between $0.5G_0$ and $1G_0$ are obtained in the γ region. The precise conductance values depend on the specific tip and are reproducible for a given tip. Importantly, for every tip the contact conductance is lower in β than in γ. In a rim around the α region (δ) a smooth transition from tunneling to contact occurs. Conductances are higher than at α positions, and the conductance rises well above the exponentially extrapolated tunneling conductance. In all parts of the unit cell the conductance keeps increasing at a rate which is tip dependent upon approaching the tip beyond the formation of a contact.

A jump to contact is typically observed in similar experiments on noble metal surfaces [18,26], where atoms are transferred from the tip to the sample. In contrast, no material transfer is observed in contacting any region of the graphene moiré unit cell. Moreover, the tip is not altered after such a contact experiment, as inferred from identical topographs recorded before and after contact experiments. The jump to contact, therefore, appears to essentially reflect an elastic deformation of the graphene layer and the tip. The conductances measured from epitaxial graphene may be compared to values from molecular junctions. The conductance of a single atom contact to a C_{60} molecule on Cu(100) [27,28] is similar to the conductance at α positions observed here. At the γ positions, $G \approx G_0$ approaches values reported from a Pt-benzene-Pt junction [29].

To gain further insight into the variation of the contact conductances, a chain model was employed to calculate conductances for different regions of the moiré unit cell (Fig. 2). For the transport calculations the TRANSIESTA package [30,31] was used. The substrate was modeled by a semi-infinite chain of Ru atoms, separated by 2.724 Å from each other, which is the Ru nearest neighbor distance in bulk material. Graphene was modeled by a (4×4) periodic graphene patch perpendicular to the Ru chain (with the chain below the center of a C ring) at three

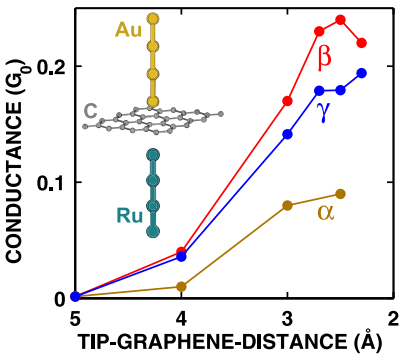

FIG. 2 (color online). Zero-bias conductance through a graphene sheet calculated from a chain model (inset). Conductances were evaluated at three Ru-graphene distances, which were determined from large-scale DFT calculations [25] of the moiré pattern. For each graphene-Ru distance the graphene-Au distance was varied to mimic the experiments. The sequence of conductances observed in the experiments [α, γ, β in Fig. 1(b)] is reproduced.

different separations to mimic the different regions of the moiré unit cell (α, β, γ). The graphene-Ru distances were obtained from large-scale DFT calculations of the whole moiré unit cell [25]. The tip was modeled by a semi-infinite chain of Au atoms (spaced by 2.949 Å), collinear to the Ru chain above the graphene patch at varying distances, to mimic the tip approach. The zero-bias conductance was calculated for the three graphene-Ru distances and a number of graphene-tip distances. The sequence of conductances observed in the experiment [α, γ, β in Fig. 1(b)] is reproduced from this model. As the model reduces the differences of the moiré regions to different graphene-Ru distances, the variation of the contact conductance can be partially attributed to this effect.

To further investigate the intriguing jump to contact behavior in β and γ, experiments with atomic precision were performed. Figure 3 shows conductance versus tip displacement curves obtained at different atomic positions in γ. While the positions of the C atoms at hcp sites of Ru (0001) (hcp-C) are directly observable in the STM topograph (Fig. 3, inset), the positions of the C atoms at the top sites (top-C) were obtained as follows. The graphene unit cell contains two C atoms, defining two hexagonal sublattices, A and B. C atoms of sublattice A (B) are at hcp (top) sites in γ and at top (fcc) sites in β. Thus, by expanding sublattice A, which is visible in β, over region γ, the positions of top-C in that region are known. While the contact conductances are similar within 10% regardless of the precise position of the measurement, the tip displacement at which contact is formed varies strongly. A jump to contact occurs at significantly smaller tip displacements (Δz) when contacting hcp-C as compared to other positions. Measurements performed at significantly higher time resolutions show that the transition occurs on a time scale of less than 500 ns, which corroborates the interpretation of the jump to contact in terms of a sudden rearrangement of atomic positions [18].

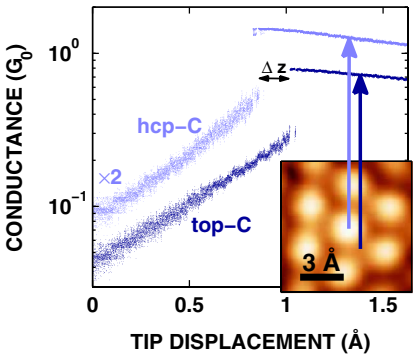

FIG. 3 (color online). Conductance versus tip displacement curves (100 mV), obtained with atomic lateral precision at the indicated positions in the γ region. The tip was approached over 50 steps in ≈ 0.5 s, and the current was recorded at a sampling frequency of 1 MHz. For clarity, only 1 out of 30 data points is shown. Inset: atomically resolved constant-current STM image of γ. While similar contact conductances are found throughout γ ($0.72G_0$ for top-C and $0.78G_0$ for hcp-C), the jump to contact occurs at distinctly different tip displacements, with a $\Delta z \approx 0.2$ Å offset between the indicated positions. Experiments at β yielded similar results. Some oscillations between tunneling and contact are attributed to small mechanical vibrations of the STM.

To address the nanomechanics involved, DFT calculations of the entire contact (tip, graphene, and three-layer slab of Ru) were performed (Fig. 4). Zero tip displacement is defined by the largest calculated tip-sample separation. Like in the experiments, a reduction of this separation is defined as positive tip displacement. When approaching the tip above hcp-C (red dot, directly below the tip, left panels), this atom moves up towards the tip by more than 0.4 Å, while the height of the neighboring top-C (orange circle) is only slightly disturbed. The bond length between the tip-apex atom and hcp-C corresponds to the average Au-Au and C-C bond length, when the hcp-C atom is lifted up; thus, we associate this lifting with contact formation. This happens at tip displacements below 1 Å. Approaching above top-C (right panels) or at the center of a C ring (not shown), the tip-apex atom moves sideways towards hcp-C and forms a contact to it. Hcp-C is pulled upwards to the tip by more than 0.2 Å during this process, at tip displacements above 2 Å. Top-C itself, however, first slightly

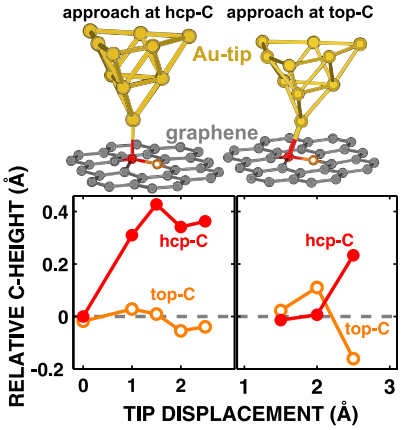

FIG. 4 (color online). Top diagrams: Relaxed structures of graphene and Au tip contacting the γ region at hcp-C (left diagram, red dot, directly below the tip) and at top-C (right diagram, orange circle) as calculated by DFT for the whole moiré unit cell including a three-layer Ru slab, graphene, and the tip. These geometries show the maximum C-atom elevation. Bottom diagrams: Heights of hcp-C (red dots) and top-C (orange circles) relative to the height of hcp-C for zero tip displacement (defined as the largest calculated tip-sample separation). Approaching the tip above hcp-C, hcp-C is lifted while top-C moves slightly. Approaching above top-C, the tip bends sideways towards hcp-C, which in turn moves up and forms the contact. Simultaneously, top-C is repelled. A tip approach towards hcp-C leads to significant lifting of hcp-C for a tip displacement below 1 Å, while this displacement exceeds 2 Å for an approach towards top-C.

moves upwards, but then is repelled as the tip bends sideways and a bond between the tip and hcp-C is formed. We associate the upwards movement of hcp-C with the jump to contact in the experiments. Thus, the jump to contact at larger tip-sample separation at the hcp-C position is reproduced by the calculations. Despite this qualitative agreement, there are quantitative differences. While the jump to contact at top-C and hcp-C sites occurs at tip-sample distances differing by more than 1 Å in the calculations, this difference is smaller in the experiments ($\Delta z \approx 0.2$ Å, with tip-dependent variations).

The results may be discussed in terms of local variations of the chemical reactivity towards the Au tip. Enhanced reactivity, i.e., the affinity to form a chemical bond, is sharply localized to C atoms at hcp or fcc sites of Ru (0001). This enhancement results from the varying hybridization of C atoms at different unit cell positions [25,32]. In low regions of the moiré pattern the top-C atoms bind strongly to the surface, transforming the hybridization of the graphene orbitals from sp^2 to sp^3 and fully occupying them. This leaves a dangling bond at the hcp-C (fcc-C), as revealed by electronic structure calculations [25]. Such dangling bonds correspond to a localized chemical reactivity [33]. The motion of hcp-C (fcc-C) towards a tip atom is facilitated as this motion drives its bond angles in the graphene layer towards tetrahedral sp^3 angles. In the high regions the short-range effect of Ru(0001) is limited and the sp^2 hybridization of graphene is unchanged; thus, no enhanced chemical reactivity can be observed.

In conclusion, graphene on Ru(0001) shows strong lateral inhomogeneities of contact formation and contact conductance in STM experiments over the moiré unit cell. These variations were analyzed by calculations of the geometric structure and the electron transport. We find that a contact is always formed to those C atoms which reside on hollow sites of the Ru (hcp-C and fcc-C), which reflects a locally enhanced chemical reactivity at these C atoms. The contact conductance modulation over the moiré unit cell is shown to result from the variation of the graphene-Ru distance within the unit cell, revealing the active role of the underlying Ru surface in locally changing the hybridization of the graphene atoms.

We acknowledge financial support from the Spanish MICINN (No. FIS2009-12721-C04-01). B. Wang's work is supported by the European Commission through the Early Stage Researcher Training Network MONET, MEST-CT-2005-020908.

Funding by the Deutsche Forschungsgemeinschaft (SFB 677) and Schleswig-Holstein-Fonds is acknowledged.

*altenburg@physik.uni-kiel.de

[1] K. S. Novoselov *et al.*, Science **306**, 666 (2004).
[2] K. S. Novoselov *et al.*, Nature (London) **438**, 197 (2005).
[3] K. S. Novoselov *et al.*, Proc. Natl. Acad. Sci. U.S.A. **102**, 10451 (2005).
[4] Y. Zhang, Y.-W. Tan, H. L. Stormer, and P. Kim, Nature (London) **438**, 201 (2005).
[5] C. Berger *et al.*, Science **312**, 1191 (2006).
[6] I. Pletikosić *et al.*, Phys. Rev. Lett. **102**, 056808 (2009).
[7] A. Nagashima, N. Tejima, and C. Oshima, Phys. Rev. B **50**, 17487 (1994).
[8] W. Moritz *et al.*, Phys. Rev. Lett. **104**, 136102 (2010).
[9] S. Marchini, S. Günther, and J. Wintterlin, Phys. Rev. B **76**, 075429 (2007).
[10] A. B. Preobrajenski, M. L. Ng, A. S. Vinogradov, and N. Mårtensson, Phys. Rev. B **78**, 073401 (2008).
[11] J. Wintterlin and M.-L. Bocquet, Surf. Sci. **603**, 1841 (2009).
[12] A. L. Vázquez de Parga *et al.*, Phys. Rev. Lett. **100**, 056807 (2008).
[13] B. Borca *et al.*, Semicond. Sci. Technol. **25**, 034001 (2010).
[14] P. W. Sutter, J.-I. Flege, and E. A. Sutter, Nature Mater. **7**, 406 (2008).
[15] K. Donner and P. Jakob, J. Chem. Phys. **131**, 164701 (2009).
[16] Y. Pan *et al.*, Appl. Phys. Lett. **95**, 093106 (2009).
[17] Z. Zhou, F. Gao, and D. W. Goodman, Surf. Sci. **604**, L31 (2010).
[18] L. Limot *et al.*, Phys. Rev. Lett. **94**, 126102 (2005).
[19] J. Kröger, N. Néel, and L. Limot, J. Phys. Condens. Matter **20**, 223001 (2008).
[20] L. Olesen *et al.*, Phys. Rev. Lett. **76**, 1485 (1996).
[21] G. Kresse and J. Hafner, Phys. Rev. B **47**, 558 (1993).
[22] P. E. Blöchl, Phys. Rev. B **50**, 17953 (1994).
[23] G. Kresse and D. Joubert, Phys. Rev. B **59**, 1758 (1999).
[24] J. P. Perdew, K. Burke, and M. Ernzerhof, Phys. Rev. Lett. **77**, 3865 (1996).
[25] B. Wang *et al.*, Phys. Chem. Chem. Phys. **10**, 3530 (2008).
[26] J. Kröger *et al.*, New J. Phys. **11**, 125006 (2009).
[27] N. Néel, J. Kröger, L. Limot, and R. Berndt, Nano Lett. **8**, 1291 (2008).
[28] N. Néel *et al.*, Phys. Rev. Lett. **98**, 065502 (2007).
[29] M. Kiguchi *et al.*, Phys. Rev. Lett. **101**, 046801 (2008).
[30] M. Brandbyge *et al.*, Phys. Rev. B **65**, 165401 (2002).
[31] J. L. Mozos *et al.*, Nanotechnology **13**, 346 (2002).
[32] B. Wang, S. Günther, J. Wintterlin, and M.-L. Bocquet, New J. Phys. **12**, 043041 (2010).
[33] R. Wolkow and Ph. Avouris, Phys. Rev. Lett. **60**, 1049 (1988).